

# 1 First measurement of heavy flavour femtoscopy in Au+Au 2 collisions at $\sqrt{s_{\text{NN}}} = 200$ GeV by STAR

3 *Priyanka Roy Chowdhury*<sup>1,\*</sup> (for the STAR Collaboration)

4 <sup>1</sup>Warsaw University of Technology, Faculty of Physics, Koszykowa 75, 00-662 Warsaw, Poland

5 **Abstract.** In the very beginning stages of heavy-ion collisions, hard par-  
6 tonic scatterings yield heavy quarks, which go through the entire Quark-Gluon  
7 Plasma medium evolution. Femtoscopic correlation is characterized as a two  
8 particle correlation at low relative momentum that depends on the size of the  
9 region from which the correlated particles emit and the final-state interaction.  
10 Such correlations between identifiable charged hadrons and charmed mesons  
11 could provide insights into their interactions with the medium and charm quarks  
12 in the hadronic phase. We describe the first femtoscopic correlation measure-  
13 ments made by the STAR experiment between  $D^0/\bar{D}^0 - \pi^\pm$ ,  $D^0/\bar{D}^0 - K^\pm$  and  
14  $D^0/\bar{D}^0 - p^\pm$  pairs at mid-rapidity in Au+Au collisions at  $\sqrt{s_{\text{NN}}} = 200$  GeV.  
15 The discussion of the physics consequences involves a comparison to theory  
16 calculations.

## 17 1 Introduction

18 In the early stages of relativistic collisions involving heavy ions, heavy quarks such as the  
19 charm ( $c$ ) and its charge conjugate ( $\bar{c}$ ) are created. Probing all stages of the evolution of  
20 heavy-ion collisions by heavy-quarks, such as Quark-Gluon-Plasma (QGP), chemical freeze-  
21 out, hadronization, kinetic freeze-out, and subsequent interactions leading to the final state,  
22 is made possible by their early establishment [1]. The study of QGP contributes to our under-  
23 standing of the universe's space-time evolution in the microseconds following the Big Bang.  
24 One heavy ( $c/\bar{c}$ ) and one light ( $(\bar{u}/u)$ ) quark make up  $D^0/\bar{D}^0$  mesons (lifetime,  $c\tau \approx 123$   
25  $\mu\text{m}$  [2]). These charmed mesons are useful to probe how heavy quarks interact with medium.  
26 The STAR experiment at RHIC (Relativistic Heavy Ion Collider) observed significant  $D^0$  el-  
27 liptic flow [3] and  $D^0$  suppression at high  $p_T$  [4] in heavy-ion collisions. Numerous theoret-  
28 ical models with varying assumptions were able to quantitatively describe these findings. In  
29 order to improve our comprehension of heavy quarks ( $c, b$ ) interactions with the medium, new  
30 observables like the two-particle momentum correlation functions are of particular interest.  
31 Phase-space evolution of emission source and final-state interactions of heavy-ion collisions,  
32 both can be studied with such measurements [5]. According to theory, phase-space cloud of  
33 outgoing correlated pairs or so-called area of homogeneity is responsive to QGP dynamics,  
34 such as collective flow [5, 6]. Size of area of homogeneity is substantially lower than the size  
35 of fireball in cases of strong correlation [5].

36 According to Koonin-Pratt equation [5], femtoscopic correlation function,  $C(k^*) =$   
37  $\int S(r)|\psi(k^*, r)|^2 d^3r$ , is a combination of emission source function,  $S(r)$  and pair-wave func-

---

\*e-mail: priyanka.roy\_chowdhury.dokt@pw.edu.pl

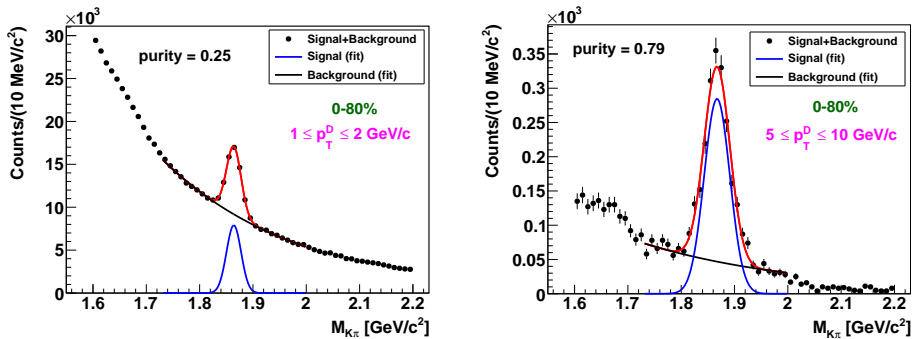
38 tion,  $\psi(k^*, r)$ . Here  $k^*$  represents the reduced momentum difference between correlated par-  
 39 ticle pairs emitting from a source of size  $r$ . We computed  $C(k^*)$  by taking the  $k^*$  ratio of  
 40 correlated [ $A(k^*)$ ] and uncorrelated [ $B(k^*)$ ]  $D^0$ -hadron pairs in the rest frame of their center  
 41 of mass given in Eq. 1 [5].

$$C(k^*) = N \frac{A(k^*)}{B(k^*)} \quad \text{and} \quad k^* = \frac{1}{2}(p_1 - p_2), \quad (1)$$

42 where  $N$  is normalization factor and  $p_1, p_2$  are momenta of  $D^0/\bar{D}^0$  and  $K/\pi/p$  tracks in the  
 43 pair-rest frame. Two tracks were chosen from the same event in order to compute  $A(k^*)$ .  $B(k^*)$   
 44 was calculated using event mixing technique to select a pair of tracks from different events  
 45 chosen within a similar primary  $z$ -vertex position ( $V_z$ ) and centrality range as the same-event  
 46 pairs.

## 47 2 $D^0/\bar{D}^0$ reconstruction and signal purity estimation

48 STAR is made up of multiple detectors with distinct functions [7]. The two primary detec-  
 49 tors for tracking and identifying charge particles are the Time Projection Chamber (TPC) and  
 50 Time of Flight (TOF). We used both TPC and TOF to select the primary tracks of considered  
 51 charged hadrons ( $\pi, K$  and  $p$ ). The HFT detector with outstanding track pointing resolu-  
 52 tion was used for the reconstruction of  $D^0/\bar{D}^0$  mesons via the  $K^\mp\pi^\pm$  decay channel with a  
 53 branching ratio of 3.89% and set of topological criteria [4]. Using STAR data from Au+Au  
 54 collisions at  $\sqrt{s_{NN}} = 200$  GeV, Fig. 1 displays the reconstructed  $D^0$  and  $\bar{D}^0$  invariant mass  
 55 distributions covering a range of 1.82 -1.91 GeV/ $c^2$  [4]. We selected  $D^0$  candidates (and their  
 56 charge conjugates) for this study based on two criteria:  $p_T > 1$  GeV/ $c$  and the ratio of signal-  
 57 to-combinatorial background under  $D^0$  peak ( $S/B$ ) had to exceed 30% in the lowest  $p_T$  bin.  
 58 With rising transverse momentum,  $p_T$ , the  $S/B$  ratio increases. The  $D^0$  signal purity ( $\frac{S}{S+B}$ )  
 59 was calculated for each  $p_T$  bin (1-2, 2-3, 3-5, and 5-10 GeV/ $c$ ). In the lowest  $p_T$  bin, the  
 purity is 25%, gradually increasing to 80% in the highest  $p_T$  bin.



60 **Figure 1.** Invariant mass ( $M_{K\pi}$ ) of  $D^0$  and  $\bar{D}^0$  candidates using STAR Run 2014 data. The black solid  
 circles depict the  $D^0$  ( $\bar{D}^0$ ) signal from same-event (SE) unlike-sign (US) pairs mixed with combinatorial  
 background from SE like-sign (LS) pairs. The red curve corresponds to a Gaussian fit of the  $D^0$  ( $\bar{D}^0$ )  
 signal, while the black line shows an exponential fit to the background. The blue curve illustrates the  
 fit to the  $D^0$  ( $\bar{D}^0$ ) signal after subtracting the SE, LS distributions within the mass range of 1.73 to 2.0  
 GeV/ $c^2$ .

## 61 3 Correlation function calculation

62 The correlation function's computed value may be impacted by incorrectly identifying cor-  
 63 related pairs. We eliminated splitted hadron tracks and excluded self-correlation between  $D^0$

64 daughters in order to reduce the potential effects of the TPC detector. Combining two differ-  
 65 ent tracks into one is another possible detector impact, however our investigation showed that  
 66 the contribution from merged tracks was negligible. To eliminate the contribution from the  
 67 background under  $D^0$  signal peak and reduce contamination of the identified hadron sample  
 68 with other particles present in the system, we implemented a purity correction for  $D^0$ -hadron  
 69 pairs using a specific formula [8]:

$$C(k^*) = \frac{C_{\text{measured}}(k^*) - 1}{\text{Pair Purity}} + 1, \quad (2)$$

70 where  $C(k^*)$  is the final correlation function after purity correction,  $C_{\text{measured}}(k^*)$  represents  
 71 the correlation function after correcting possible detector effects, while Pair Purity is deter-  
 72 mined by multiplying the  $D^0$  signal purity with the average purity of the hadron sample. The  
 73 purity of the hadron sample was determined by performing corresponding  $n\sigma$  fit in differ-  
 74 ent momentum bins, utilizing the sum of Gaussian functions associated with other hadrons  
 75 and electrons present in the system. Hadrons were selected with momentum criteria,  $p_\pi <$   
 76  $1 \text{ GeV}/c$ ,  $p_p < 1.2 \text{ GeV}/c$  and  $p_K < 1 \text{ GeV}/c$  as they become difficult to distinguish from  
 77 electrons and other hadrons beyond the mentioned thresholds respectively. Within selected  
 78 momentum range, average purity of  $\pi$  and  $p$  are  $(99.5 \pm 0.5)\%$  while for  $K$  sample, purity is  
 79  $(97 \pm 3)\%$ . Systematic uncertainty studies were made by variations in the topological cuts  
 80 used for  $D^0$  reconstruction [4], and by including the uncertainties in the purity estimation of  
 81  $D^0$ -hadron pairs.

## 82 4 Results and discussions

83 Figure 2 presents the final correlation function of  $D^0/\bar{D}^0 - \pi^\pm$ ,  $D^0/\bar{D}^0 - p^\pm$  and  $D^0/\bar{D}^0 - K^\pm$   
 84 pairs using STAR data from minimum bias Au+Au collision at  $\sqrt{s_{\text{NN}}} = 200 \text{ GeV}$  within  
 85  $|\eta| < 1$ . The  $C(k^*)$  distribution is consistent with unity, indicating an absence of significant  
 86 correlation, with large statistical fluctuations. The strength of the correlation is linked to the  
 size of the source [5, 6]. A weak or absent correlation suggests that the emission source

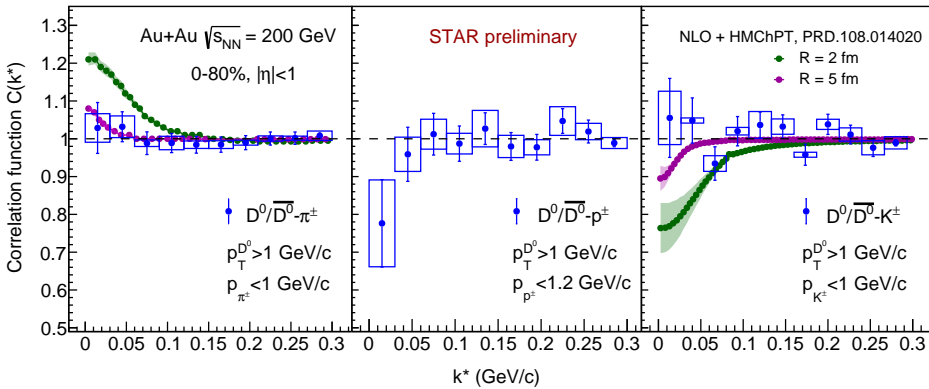


**Figure 2.**  $C(k^*)$  for (left)  $D^0/\bar{D}^0 - \pi^\pm$ , (mid)  $D^0/\bar{D}^0 - p^\pm$  and (right)  $D^0/\bar{D}^0 - K^\pm$  pairs. The blue solid circles, along with the boxes, indicate the STAR data and the associated systematic uncertainties. The green and pink bands illustrate the  $C(k^*)$  values predicted by NLO + HMChPT model for source sizes of 2 fm and 5 fm, respectively.

87

88 from which the  $D$ -hadron pairs are produced is relatively large in size. In left and right panel,

89 STAR data are compared with  $C(k^*)$  calculated using NLO (next-to-leading order)-HMChPT  
90 (Heavy Meson Chiral Perturbation Theory) scheme [9–11]. Theory calculations considered  
91 a mixture of (left)  $D^0 - \pi^+$  and  $D^+ - \pi^0$  pairs while (right)  $D^0 - K^+$  pairs [9]. Neither of  
92 these channels includes Coulomb interaction. The STAR data and theoretical predictions  
93 align with an emission source size of 5 fm or more. The  $D^0 K^+$  channel exhibits a threshold  
94 near 0.083 GeV where a cusp effect is observed. The prediction shows a marked depletion at  
95 the origin, which is attributed to the  $D_s^*(2317)^\pm$  bound state and becomes more pronounced  
96 as the source radius decreases [9]. However, the resonance effect of this state is not evident in  
97 the STAR results due to either the large source size or significant experimental uncertainties.  
98 As a next step, we plan to update these results by combining data from Runs 2014 and 2016.  
99 This approach is expected to improve the precision of the correlation function measurements  
100 and offer more definitive conclusions about the source size. Additionally, theoretical inputs  
101 are necessary for a better interpretation of these data.

## 102 5 Acknowledgement

103 Priyanka Roy Chowdhury expresses gratitude for the financial support provided by the Na-  
104 tional Science Centre, Poland (NCN) under grant no. 2018/30/E/ST2/0008, as well as partial  
105 support from the U.S. Department of Energy (DOE).

## 106 References

- 107 [1] X. Dong *et al.*, Open Heavy-Flavor Production in Heavy-Ion Collisions, *Ann. Rev. Nucl.*  
108 *Part. Sci.* **69**, 417-445 (2019).
- 109 [2] R. L. Workman *et al.* [Particle Data Group], Review of Particle Physics, *PTEP* **2022**,  
110 083C01 (2022).
- 111 [3] L. Adamczyk *et al.* [STAR], Measurement of  $D^0$  Azimuthal Anisotropy at Midrapidity  
112 in Au+Au Collisions at  $\sqrt{s_{NN}}=200$  GeV, *Phys. Rev. Lett.* **118**, no.21, 212301 (2017).
- 113 [4] J. Adam *et al.* [STAR], Centrality and transverse momentum dependence of  $D^0$ -meson  
114 production at mid-rapidity in Au+Au collisions at  $\sqrt{s_{NN}} = 200$  GeV, *Phys. Rev. C* **99**,  
115 no.3, 034908 (2019).
- 116 [5] M. A. Lisa *et al.*, Femtoscopy in relativistic heavy ion collisions, *Ann. Rev. Nucl. Part.*  
117 *Sci.* **55**, 357-402 (2005).
- 118 [6] S. V. Akkelin and Y. M. Sinyukov, The HBT interferometry of expanding sources, *Phys.*  
119 *Lett. B* **356**, 525-530 (1995).
- 120 [7] Special Issue on RHIC and Its Detectors, edited by M. Harrison, T. Ludlam and S. Ozaki,  
121 *Nucl. Instrum. Methods Phys. Res., Sect. A* **499**, no.2–3 (2003).
- 122 [8] J. Adams *et al.* [STAR], Proton - lambda correlations in central Au+Au collisions at  
123  $S(NN)^{1/2} = 200$ -GeV, *Phys. Rev. C* **74**, 064906 (2006).
- 124 [9] M. Albaladejo, J. Nieves and E. Ruiz-Arriola, Femtosopic signatures of the lightest S-  
125 wave scalar open-charm mesons, *Phys. Rev. D* **108**, no.1, 014020 (2023).
- 126 [10] F. K. Guo, C. Hanhart and U. G. Meissner, Interactions between heavy mesons and  
127 Goldstone bosons from chiral dynamics, *Eur. Phys. J. A* **40**, 171-179 (2009).
- 128 [11] L. S. Geng, N. Kaiser, J. Martin-Camalich and W. Weise, Low-energy interactions of  
129 Nambu-Goldstone bosons with  $D$  mesons in covariant chiral perturbation theory, *Phys.*  
130 *Rev. D* **82**, 054022 (2010).